ISSN 1063-7761, Journal of Experimental and Theoretical Physics, 2008, Vol. 106, No. 2, pp. 347–354. © Pleiades Publishing, Inc., 2008.
Original Russian Text © L.V. Zorina, T.G. Prokhorova, S.V. Simonov, S.S. Khasanov, R.P. Shibaeva, A.I. Manakov, V.N. Zverev, L.I. Buravov, and É.B. Yagubskiĭ, 2008, published in Zhurnal Éksperimental'noĭ i Teoreticheskoĭ Fiziki, 2008, Vol. 133, No. 2, pp. 403–411.

ELECTRONIC PROPERTIES OF SOLIDS

Structure and Magnetotransport Properties of the New Quasi-Two-Dimensional Molecular Metal β''-(BEDT–TTF)$_4$H$_3$O[Fe(C$_2$O$_4$)$_3$] · C$_6$H$_4$Cl$_2$

L. V. Zorina[a, *], T. G. Prokhorova[b], S. V. Simonov[a, **], S. S. Khasanov[a], R. P. Shibaeva[a], A. I. Manakov[a], V. N. Zverev[a], L. I. Buravov[b], and É. B. Yagubskiĭ[b]

[a] *Institute of Solid State Physics, Russian Academy of Sciences, Chernogolovka, Moscow oblast, 142432 Russia*
[b] *Institute of Problems of Chemical Physics, Chernogolovka Branch, Russian Academy of Sciences, Chernogolovka, Moscow oblast, 142432 Russia*
**e-mail: zorina@issp.ac.ru*
***e-mail: simonovsv@rambler.ru*

Received July 20, 2007

Abstract—The β''-(BEDT–TTF)$_4$A^I[M^{III}(C$_2$O$_4$)$_3$] · G (A^I = NH_4^+, H_3O^+, K^+, Rb^+; M^{III} = Fe, Cr; G = "guest" solvent molecule) family of layered molecular conductors with magnetic metal oxalate anions exhibits a pronounced dependence of the conducting properties on the type of neutral solvent molecules introduced into the complex anion layer. A new organic dichlorobenzene (C$_6$H$_4$Cl$_2$)-containing conductor of this family, namely, β''-(BEDT–TTF)$_4$H$_3$O[Fe(C$_2$O$_4$)$_3$] · C$_6$H$_4$Cl$_2$, is synthesized. The structure of the synthesized single crystals studied by X-ray diffraction is characterized by the following parameters: a = 10.421(1) Å, b = 19.991(2) Å, c = 35.441(3) Å, β = 92.87(1)°, V = 7374(1) Å^3, space group $C2/c$, and Z = 4. In the temperature range 0.5–300 K, the conductivity of the crystals is metallic without changing into a superconducting state. The magnetotransport properties of the crystals are examined in magnetic fields up to 17 T at T = 0.5 K. In fields higher than 10 T, Shubnikov–de Haas oscillations are detected, and the Fourier spectrum of these oscillations contains two frequencies with maximum amplitudes of about 80 and 375 T. The experimental results are compared with the related data obtained for other phases of this family. The possible structural mechanisms of the effect of a guest solvent molecule on the transport properties of the β''-(BEDT–TTF)$_4$A^I[M^{III}(C$_2$O$_4$)$_3$] · G crystals are analyzed.

PACS numbers: 61.10.Nz, 61.66.Hq, 73.43.Qt
DOI: 10.1134/S1063776108020131

1. INTRODUCTION

The molecular conductors based on the radical cation salts of organic π donors are characterized by a high anisotropy of their conducting properties and a wide spectrum of the collective electron states characteristic of low-dimensional systems. [1].

The radical cation salts of the β''-(BEDT–TTF)$_4$A^I[M^{III}(C$_2$O$_4$)$_3$] · G (A^I = NH_4^+, H_3O^+, K^+, Rb^+; M^{III} = Fe, Cr; G = "guest" solvent molecule) family with metal oxalate anions are of particular interest for researchers in the field of low-dimensional molecular conductors, since they contain the functional anion complexes of paramagnetic metals [M^{III}(C$_2$O$_4$)$_3$]$^{3-}$ apart from the conducting radical cation layers of bis(ethylenedithio)tetrathiafulvalene (BEDT–TTF). As a result, a combination of conducting and magnetic properties can be obtained in one molecular crystal. The crystals of this family have been extensively studied since the discovery of the first organic superconductor β''-(BEDT–TTF)$_4$H$_3$O[Fe^{III}(C$_2$O$_4$)$_3$] · BN (BN = benzonitrile) containing paramagnetic 3d centers. It has T_c = 8.5 K and a very weak antiferromagnetic interaction between the spin moments of neighboring Fe^{III} ions [2, 3]. The family of isomorphic β'' phases with paramagnetic (Fe^{III}, Cr^{III}) and diamagnetic (Ga^{III}) ions and various molecular solvents was then grown. These solvents were benzonitrile [4–7], nitrobenzene (NB) [8–11], pyridine (PYR) [10–13], dichloromethane (DCM) [13, 14], dimethylformamide (DMF) [15–17], chlorobenzene (CB) [13, 18], and bromobenzene (BB) [18, 19]. The conducting properties of these compounds were found to be diverse and to vary from metallic to semiconducting properties despite the fact that they have a similar structure.

The presence of a relation between the sizes of the solvent molecules that enter into the complex anion layer and the electron transport is beyond question. Superconducting crystals include large solvent crystals, and the superconducting transition temperature

increases with the solvent molecule size. These crystals exhibit Shubnikov–de Haas magnetic oscillations at one or two frequencies [20–23]. Superconductivity is often preceded by a complex temperature dependence of the electrical resistance with a broad minimum in the range 40–150 K in various phases [21, 22]. Below this temperature, the resistance increases slowly, which is related to partial charge localization [22], and the increase in the resistance is then changed by a sharp decrease in a superconducting state. The phases containing small solvent molecules have no superconducting transition but exhibit Shubnikov–de Haas oscillations. However, these oscillations result from a combination of a large number of frequencies, which corresponds to a more complex Fermi surface [24–26].

The authors of [26] believe that the effect of introduction of different solvents into the anion metal oxalate is similar to the effect of chemical pressure, which is determined by the guest solvent molecule volume. However, structural data indicate that the structural effects induced by the substitution of a solvent are more complex (below, they will be considered in detail) and that the character of electronic states most strongly depends on the solvent linear size along one of the unit cell directions rather than on the solvent volume [16]. The new organic conductor β"-(BEDT–TTF)$_4$H$_3$O[Fe(C$_2$O$_4$)$_3$] · C$_6$H$_4$Cl$_2$, which is studied in this work, contains dichlorobenzene (DCB). The DCB molecule has the largest volume among all the solvents used earlier to synthesize β"-(BEDT–TTF)$_4$A^{I}[M^{III}(C$_2$O$_4$)$_3$] · G crystals. We investigate the structure, conducting properties, and Shubnikov–de Haas oscillations of the grown single crystals. The experimental data obtained are analyzed and compared with the results on crystals from other phases of the family that were obtained earlier by us or other researchers.

2. EXPERIMENTAL

2.1. Synthesis of β"-(BEDT–TTF)$_4$H$_3$O[Fe(C$_2$O$_4$)$_3$] · C$_6$H$_4$Cl$_2$ Crystals

The crystals were synthesized from BEDT–TTF (Aldrich), (NH$_4$)$_3$Fe(C$_2$O$_4$)$_3$ · 3H$_2$O (Aldrich), *o*-DCB (Aldrich), and ethyl alcohol (95%, used without additional purification). 18-crown-6 (Aldrich) was purified by recrystallization from acetonitrile and dried in a vacuum at a temperature of 30°C over phosphorus pentoxide (P$_2$O$_5$).

The crystals were grown upon electrochemical oxidation of BEDT–TTF (with a concentration $C = 5.2 \times 10^{-4}$ mol/l) on a platinum electrode at a direct current of 0.4 μA in a DCB + 10%C$_2$H$_5$OH solution at a temperature of 25°C. As the electrolyte, we used (NH$_4$)$_3$Fe(C$_2$O$_4$)$_3$ · 3H$_2$O ($C = 4.6 \times 10^{-3}$ mol/l) with 18-crown-6 ($C = 2.26 \times 10^{-2}$ mol/l). The crystals grew in the form of bright black bars on an anode for 20 days.

2.2. X-ray Diffraction Studies

The main crystallographic data are as follows: a = 10.421(1) Å, b = 19.991(2) Å, c = 35.441(3) Å, β = 92.87(1)°, V = 7374(1) Å^3, space group $C2/c$, the number of formula units in the unit cell is $Z = 4$ for the composition C$_{52}$H$_{39}$Cl$_2$FeO$_{13}$S$_{32}$, the formula unit weight is M = 2024.5 a.u., and the calculated density is ρ_{calc} = 1.824 g/cm^3. The electron diffraction pattern of the β"-(BEDT–TTF)$_4$H$_3$O[Fe(C$_2$O$_4$)$_3$] · C$_6$H$_4$Cl$_2$ single crystals contained 15001 reflections and was recorded on an Enraf Nonius CAD-4 diffractometer using MoK_α radiation (λ = 0.71073 Å, graphite monochromator) and ω scanning in the angular range $2° < \theta < 26°$ at room temperature. The experimental intensities were not corrected for absorption (the crystal size was 0.25 × 0.50 × 0.10 mm^3; the absorption coefficient was μ(MoK_α) = 12.43 cm^{-1}).

The structure of the crystals was determined by a direct method followed by Fourier syntheses and was then refined by the full-matrix least squares method using the SHELX97 software package [27] in the anisotropic approximation for all non-hydrogen atoms. The positions of hydrogen atoms in the ethylene groups of the BEDT–TTF donor and in the benzene solvent ring were specified geometrically using isotropic temperature factors U_{iso}(H) = 1.2U_{eq}(C), where U_{eq} is the equivalent temperature factor of the corresponding carbon atom. For the H$_3$O$^+$ cation, the positions of hydrogen atoms were found from the electron-density difference synthesis, and their coordinates were refined: U_{iso}(H) = 1.2U_{eq}(O). To refine 531 structural parameters, we used 7206 independent reflections (the factors of averaging equivalent reflections were R_{int} = 0.0353 and R_σ = 0.0445). The final reliability factors were R = 0.0348 and R_w = 0.0869 for 4965 independent reflections with $I > 2\sigma(I)$; the goodness of fit was GooF = 1.001; and the maximum and minimum residual electron densities were 0.549e/Å^3 and –0.408e/Å^3, respectively. The structural information of the synthesized compound was deposited as a CIF file at the Cambridge structural database (CCDC no. 665075).

2.3. Magnetotransport Measurements

The electrical resistance was measured using a 20-Hz alternating current, the four-probe method, and a synchronous detector. The sample for transport measurements had the form of a thin 0.5 × 0.3 × 0.1-mm plate whose surface was oriented along conducting layers. A pair of contacts was applied on either sample surface with a conducting carbon paste. The sample resistance was measured when a current passed across the conducting layers. The current through the sample did not exceed 10 μA. We failed to measure the longitudinal resistance of the sample because of its strong anisotropy. For low-temperature magnetotransport measurements, we used a cryostat with a superconducting solenoid, which created a magnetic field of up to 17 T. The

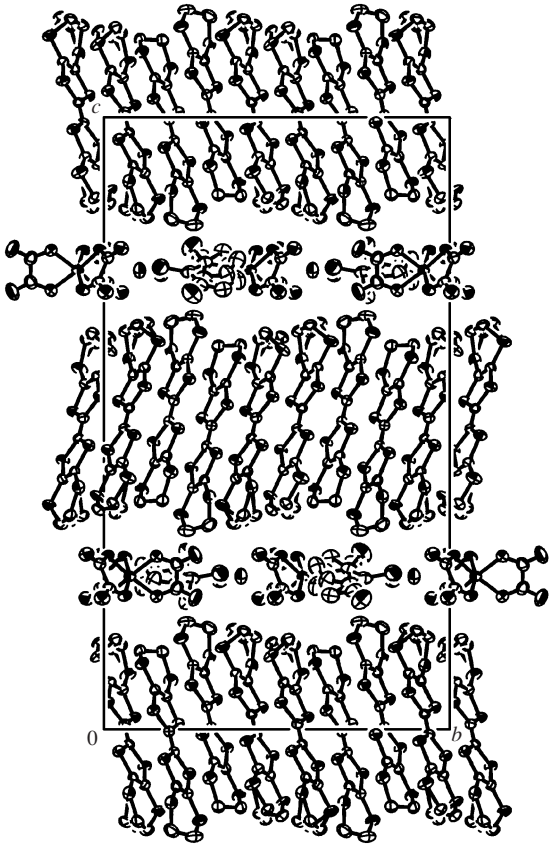

Fig. 1. Projection of the structure of β"-(BEDT–TTF)$_4$H$_3$O[Fe(C$_2$O$_4$)$_3$] · DCB along the *a* axis.

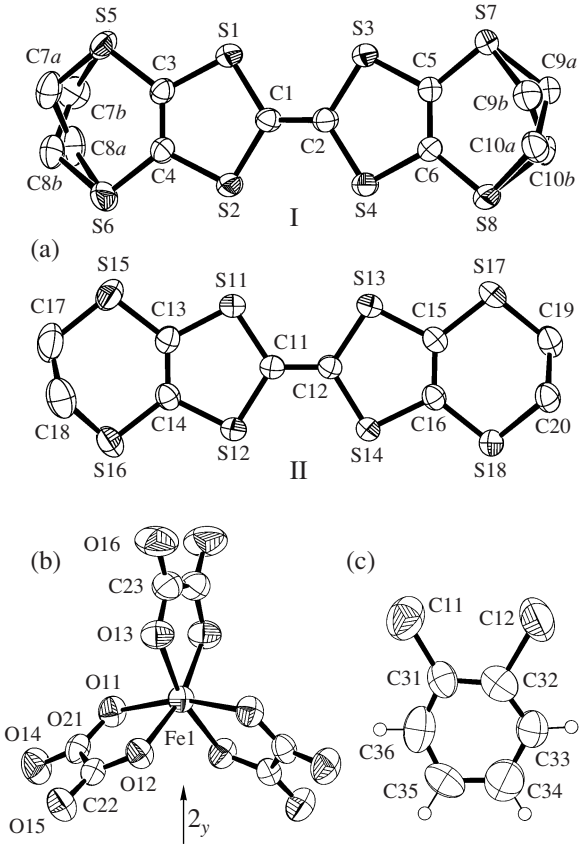

Fig. 2. Numbering of atoms in the molecules (a) BEDT–TTF I and BEDT–TTF II, (b) Fe(C$_2$O$_4$)$_3$, and (c) DCB.

field was oriented normal to the conducting layers. The sample was placed in an insert in which the vapors of liquid He^3 were pumped out; with this insert, we were able to work in the temperature range 0.5–300 K.

3. EXPERIMENTAL RESULTS

3.1. Structure of the β"-(BEDT–TTF)$_4$H$_3$O[Fe(C$_2$O$_4$)$_3$] · C$_6$H$_4$Cl$_2$ Crystal

As all crystals of the β"-(BEDT–TTF)$_4$A^{I}[M^{III}(C$_2$O$_4$)$_3$] · G family, crystals of the radical cation salt β"-(BEDT–TTF)$_4$H$_3$O[Fe(C$_2$O$_4$)$_3$] · C$_6$H$_4$Cl$_2$ has monoclinic symmetry (space group *C*2/*c*) and a layered structure (Fig. 1). Complex anion layers alternate with the conducting layers of organic donors along the *c* direction. Two crystallographically independent BEDT–TTF donors are in a general position, and the ethylene groups of one of them are disordered in two positions (Fig. 2a). The conducting organic layer has a β"-type packing (Fig. 3) and consists of stacks oriented differently (along [310] and [$3\bar{1}0$]) in neighboring layers (z = 0 and 0.5, respectively). The planes of the central TTF donor fragments are parallel to each other inside the layer and make an angle of about 65° with the BEDT–TTF molecules from the neighboring layers. The shortest and numerous intermolecular contacts (S···S = 3.399(1)–3.575(1) Å) form between the stacks

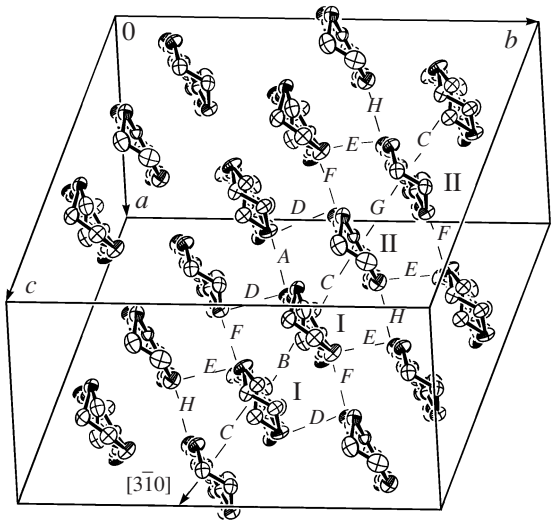

Fig. 3. Radical cation layer (z = 0.5) along the long axis of the BEDT–TTF molecule. Roman letters indicate intermolecular interactions in the layer.

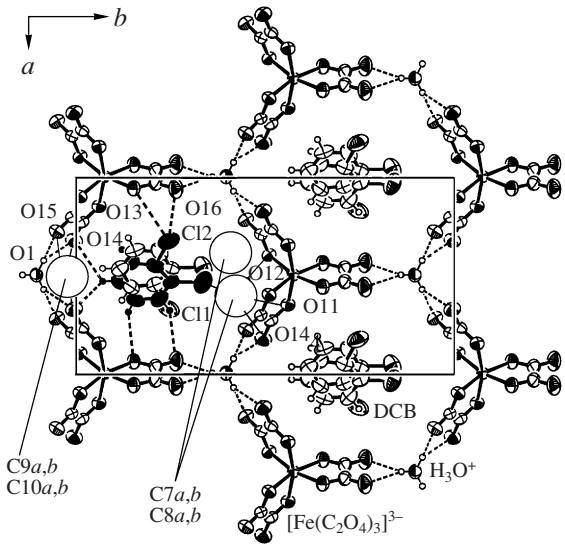

Fig. 4. Projection of the complex anion layer along the *c* direction.

in the molecular plane; these are the so-called side-by-side interactions designed by letters *A* and *F* in Fig. 3. Moreover, one short S···S contact (S···S = 3.666(1) Å) exists in a stack (interaction *C*). The distances between the planes of the TTF fragments of the neighboring donors in a stack are 3.65(3), 3.63(3), and 3.534(5) Å (interactions *B*, *C*, and *G* in Fig. 3, respectively).

Apart from the $[Fe(C_2O_4)_3]^{3-}$ anion located in the twofold axis (Fig. 2b), the complex anion layer includes a hydroxonium cation and the neutral molecules of the dichlorobenzene solvent (Fig. 2c). The structure of the layer resembles honeycomb (Fig. 4). Paramagnetic Fe^{III} ions and H_3O^+ cations alternate at the vertices of the hexagonal network, which is slightly extended along the *b* axis. The internal oxygen atoms of the C_2O_4 oxalate groups of the anion octahedrally coordinate an iron atom (the Fe–O distances are 2.005(2), 2.010(2), 2.011(2) Å), whereas the external oxygen atoms form hydrogen bonds with the hydroxonium cation. The bond geometry is given in Table 1.

Neutral solvent guest molecules occupy the hexagonal cavities of the anion layer. The set of the symmetry elements of the *o*-DCB molecule, in which chlorine atoms are connected to two neighboring vertices of a benzene ring, includes a twofold rotation axis. Nevertheless, the local symmetry elements of the solvent do not coincide with the crystal symmetry, the solvent molecule *o*-DBC is located on a general position near the 2_y axis, and one of the C–Cl bonds is directed approximately along this axis toward an iron atom. The planes of the DCB molecules occupying two positions that are equiprobable with respect to the 2_y axis are nonparallel to each other, and the angle between them is 16.1(2)°. The benzene ring lies between two oxalate groups extended along the *b* direction and are almost perpendicular to them: the angle the ring plane makes with these groups is approximately 81.8(1)°. One of the chlorine atoms (Cl2) forms shorter Cl···O contacts (2.787(5), 3.350(4) Å) with the anion oxalate group, whereas the Cl1···O distances are longer than 3.5 Å. The donor and anion layers interact through a number of the hydrogen contacts of the BEDT–TTF ethylene groups with oxygen (H···O = 2.35–2.83 Å) and chlorine (H···Cl = 2.62–2.99 Å) atoms.

3.2. Conducting Properties and Shubnikov–de Haas Oscillations

The temperature dependence of the transverse resistance *R* of the sample is shown in Fig. 5. Superconductivity has not been detected down to a minimum temperature of 0.5 K. The *R*(*T*) dependence has a positive derivative over the entire temperature range below 300 K. A short negative-derivative segment appears only at a low temperature. This segment is shown in the inset to Fig. 5. At $T < 3$ K, the *R*(*T*) dependence is seen to be well described by a logarithmic law, which suggests that the low-temperature segment with a negative slope in the *R*(*T*) dependence is related to the weak localization effect in a quasi-two-dimensional system.

Figure 6a shows the dependence of the transverse resistance of the sample on the magnetic field at 0.5 K. At low fields, a small segment with a negative magnetoresistance exists, which is thought to be related to a magnetic-field-induced break in weak localization. Shubnikov–de Haas oscillations are clearly visible in fields higher than 10 T, and their amplitude increases with the field. The oscillation period on the 1/*B* scale is 2.66×10^{-3} T^{-1}, which corresponds to a fundamental

Table 1. Geometry of the hydrogen bonds between the hydroxonium cation and the anion in β"-$(BEDT–TTF)_4H_3O[Fe(C_2O_4)_3] \cdot DCB$

D–H···*A* contact	*D*–H, Å	H···*A*, Å	*D*–H···*A* angle
O1–H1a···O16	1.08(7)	2.07(5)	139(1)°
O1–H1b···O14	1.14(4)	1.94(5)	144(3)°
O1–H1b···O15	1.14(4)	2.04(5)	128(3)°

Note: *D* and *A* are the donor and acceptor of the hydrogen bond, respectively.

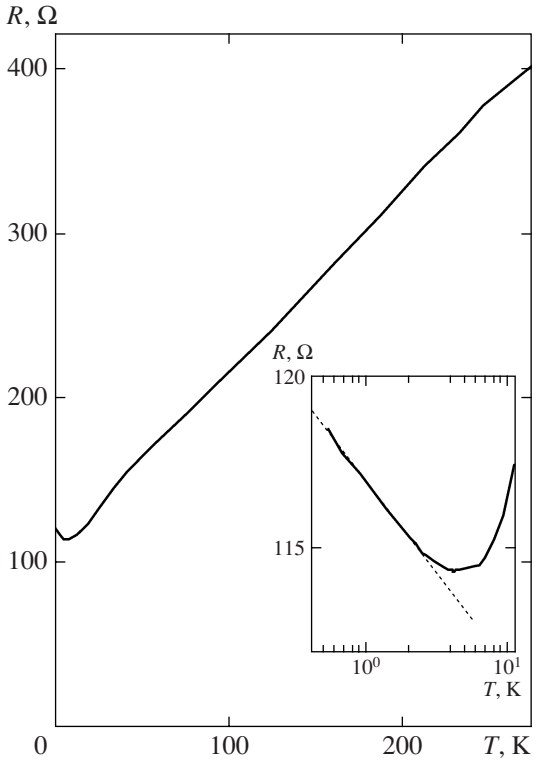

Fig. 5. Temperature dependence of the transverse resistance of β"-(BEDT–TTF)$_4$H$_3$O[Fe(C$_2$O$_4$)$_3$] · DCB. In the inset, the low-temperature segment is shown on a logarithmic temperature scale.

mode $F_1 = 376$ T. The inset to Fig. 6a also demonstrates that oscillations with a larger period (which is approximately equal to 1.2×10^{-2} T^{-1}) are also present apart from this mode, and they correspond to a fundamental mode $F_2 \approx 80$ T. Both modes are clearly visible in the Fourier spectrum of the Shubnikov–de Haas oscillations given in Fig. 6b. A more complete spectral analysis of the oscillations requires additional studies over a wider magnetic-field range.

4. DISCUSSION

As the components of the complex anion layer in the β"-(BEDT–TTF)$_4$A^{I}[M^{III}(C$_2$O$_4$)$_3$] · G family change, the following crystals can form: superconductors, stable metals, and crystals with a metal–insulator transition. When considering the structure–properties correlation, we detected a number of relations. For example, an increase in the metallic atom size increases the superconducting transition temperature T_c in the series Cr^{III}–Fe^{III}–Ga^{III}. However, the pronounced dependence of the conducting properties on the type of neutral guest solvent molecules entering into the structure of the crystal is of particular interest.

Table 2 gives the sequence of changes in the properties of the phases with the paramagnetic anion [Fe^{III}(C$_2$O$_4$)$_3$]$^{3-}$. The superconducting transition temperature is maximal ($T_c = 8.5$ K) in the parent compound of the family, which was synthesized using the BN solvent. A superconducting state in the crystals with NB and BB appears at a lower temperature (6.2 and 4.0 K, respectively). Most crystals with DMF are stable quasi-two-dimensional organic metals down to liquid-helium temperatures, and only some samples exhibit an increase in resistance as temperature decreases below 40–50 K, followed by a superconducting transition at $T_c < 2$ K. Finally, the crystals with PYR demonstrate a complex temperature dependence of the conductivity with a minimum resistance at 100–150 K and a maximum resistance at 60–80 K and, then, again metallic behavior.

The detected effect of solvent molecules on the electronic properties cannot be put equal to the chemical compression effect, since the sequence of changes in

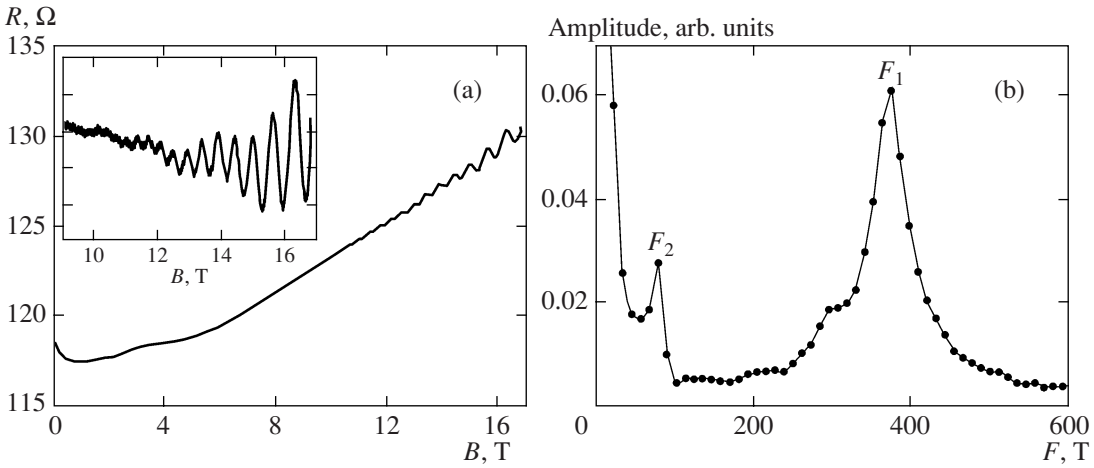

Fig. 6. (a) Magnetic-field dependence of the transverse resistance of β"-(BEDT–TTF)$_4$H$_3$O[Fe(C$_2$O$_4$)$_3$] · DCB at a temperature of 0.5 K and (b) the Fourier spectrum of the Shubnikov–de Haas oscillations in β"-(BEDT–TTF)$_4$H$_3$O[Fe(C$_2$O$_4$)$_3$] · DCB.

Table 2. Molecular conductors in the β"-(BEDT–TTF)$_4$A^I[Fe(C$_2$O$_4$)$_3$] · G family

G*	A^I	V_G, Å^3**	L_G, Å^3 †	$\alpha_{ox}^{\dagger\dagger}$	Properties☆	Reference
PYR	Rb	115	2.43	61.0°	*M–I–M*	[13]
PYR	H_3O	115	2.89	61.4°	*M–I–M*	[12, 24]
DMF	NH_4	115	3.39	62.3°	*M*, T_c < 2 K	[15, 21]
DCB	H_3O	160	4.42	64.4°	*M* (at T > 0.5 K)	This work
BB	H_3O	155	4.61	64.1°	T_c = 4.0 K	[19]
NB	H_3O	150	4.75	70.3°	T_c = 6.2 K	[9]
BN	H_3O	145	5.32	68.3°	T_c = 8.5 K	[2]

Notes: * See Fig. 7.
** The solvent molecule volume calculated from the CCDC data [28].
† The solvent molecule length along the *b* axis in the anion layer of the crystal.
†† The angle between the plane of the anion oxalate ligand and the anion-layer plane.
☆ *M*, metal; *I*, insulator (see text).

the properties does not agree with the sequence of changes in the unit cell volumes of the crystals and in the molecular volumes of the solvents. The volumes of the *G* molecules given in Table 2 were calculated from the structures of the pure solvents (*V*/*Z*) using the CCDC data [28]. In this series of solvents, the volume of the dichlorobenzene molecule is seen to be maximal; however, superconductivity in the DCB-containing crystals is not detected down to 0.5 K.

When considering the structural mechanisms of the effect of a solvent on the properties of the crystals, we conclude that the length of the solvent molecule along the *b* axis rather than its volume is important. The point is that the complex anion layer in the crystals of layered organic conductors can be considered as a supramolecular guest–host ensemble. In the crystals under study, the structure of the host is an A^I[M^{III}(C$_2$O$_4$)$_3$] anion network with large cavities. Guest–solvent molecules occupy these cavities and stabilize the structure. A solvent can occupy different positions in the cavity of the anion layer, and part of the cavity can remain unfilled. In the family under study, the shape and position of the guest molecule were found to weakly affect the structure of the host. The cavity size is controlled by the A^I and M^{III} anion sizes and weakly depends on the solvent molecule size. For example, for the crystals with Fe^{III}, the cavity area is 103 ± 1 Å^2, and the difference in the solvent volumes reaches 40–50 Å^3. Therefore, a certain unoccupied volume is retained in the cavities of the anion layer when small guest molecules are located in them. The specific features of the solvent arrangement are such that the molecule sizes along the *a* axis are similar and those along the *b* axis change significantly; as a result, the free volume in the hexagonal cavity is determined by the solvent molecule length in the *b* direction. The linear size L_G along this direction is calculated from the difference in the maximum and minimum *y* coordinates of the non-hydrogen solvent atoms with allowance for the parameter *b* of each structure (see Table 2). This parameter increases in the series PYR–DMF–DCB–BB–NB–BN, which agrees completely with the change in the properties, and the DCB molecule fits well into this sequence.

A positional disorder appears when a free space forms in the hexagonal cavities occupied by small solvent molecules, and this disorder is detected in both the donor and anion layers of the crystals. The end ethylene groups of one of the two crystallographically independent BEDT–TTF molecules are located over the cavity on either side of a solvent molecule along the *b* axis (see Fig. 4). They are disordered in all structures at room temperature; however, in molecular conductors, this is a conventional thermal disorder, which disappears at 100–150 K. In crystals with small solvent molecules (which do not transform into a superconducting state or transform into it at a very low temperature), a disorder in the conducting layer remains the same [10, 14] or even increases [12] as the temperature decreases. These crystals are characterized by disordered DCM, PYR, DMF, and DCB solvent molecules along the 2_y axis at room and lower temperatures, and only the DMF molecule has no twofold axis and cannot be ordered in the cavity of the anion layer without changing the crystal symmetry. Apart from disordering, the anion layer undergoes the rotation of the two anion oxalate groups that do not lie in the 2_y axis and are located over the free volume of the cavity (see the values of α_{ox} in Table 2), which inevitably should change the intermolecular radical cation···anion interactions. Thus, a solvent affects both the degree of disorder in the structure and the relative position of molecules in the anion and conducting donor layers.

The behavior of the electron system of β"-(BEDT–TTF)$_4$A^I[M^{III}(C$_2$O$_4$)$_3$] · G crystals is extremely sensitive to insignificant changes in the supramolecular organization, which is likely to be related to the specific features of their band structure. According to calculations for crystals with the DMF solvent [15], the Fermi level falls in a very narrow energy gap between two upper

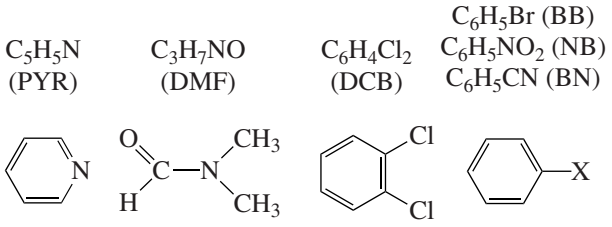

Fig. 7.

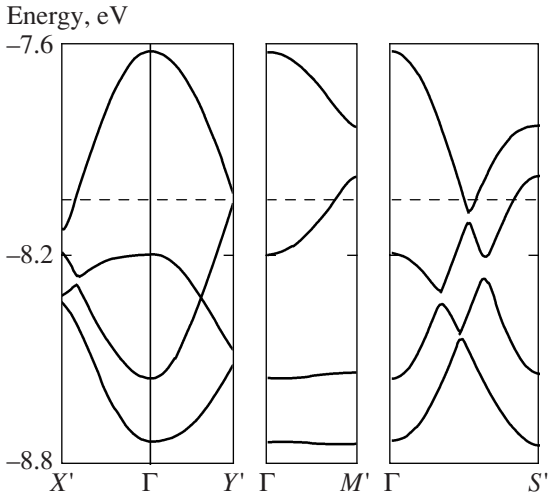

Fig. 8. Electronic band structure calculated for the donor layer of β"-(BEDT–TTF)$_4$NH$_4$[Fe(C_2O_4)$_3$] · DMF crystals [15].

bands in the band structure near a certain point (point *Y*' in Fig. 8). Therefore, even small structural variations caused by a change in the temperature, pressure, or cation–anion interactions can significantly change the shape of the Fermi surface in this region. The band calculations in [15] and the studies of the crystals of this family in magnetic fields [20–25] demonstrate that the Fermi surface consists of one or two closed orbits in the superconducting crystals of this family and that the number of orbits increases and the shape of the Fermi surface becomes more complex in the case of nonsuperconducting phases.

The temperature dependence of the resistance of the crystals of the family under study often exhibits metallic behavior with a broad minimum in the range 40–150 K (the temperature of the minimum is different in different phases), and the resistance increases slowly below this minimum. It should be noted that the dependence of the conductivity in segments with a negative derivative is in conflict with the classical semiconductor behavior. The increase in the resistance is thought to be related to partial charge localization: the Raman study of the crystals demonstrates that the peak at a frequency of 1492 cm^{-1}, which corresponds to the BEDT–TTF$^{0.5+}$ donor charge at room temperature, begins to split at 100 K [22]. The resistance of the β"-(BEDT–TTF)$_4$A^{I}[M^{III}(C_2O_4)$_3$] · G crystals usually increases before the transition into a superconducting state [18, 21, 22]; however, this resistance can also continue to increase down to the lowest temperatures [14, 18, 24], or the system can return its metallic behavior upon further cooling [13, 24]. It should be noted that our samples with the DMF or DCB solvent exhibited a monotonic and virtually linear temperature dependence of the resistance over a wide temperature range (from 5 to 300 K), which is in conflict with the nonmonotonic dependences detected in [22, 24, 26]. This conflict is likely to indicate that the electron correlations responsible for the formation of charge density waves and partial carrier localization are weakly pronounced in our samples.

The magnetotransport properties of the samples of an organic metal with Fe^{III} and the DMF solvent were studied earlier in pulsed magnetic fields as high as 55 T [21, 23]. The Fourier spectrum of the Shubnikov–de Haas oscillations exhibited two frequencies with maximum amplitudes, namely, $F_a = 48 \pm 2$ T and $F_b = 241 \pm 5$ T. These frequencies corresponded to two different closed orbits appearing in a strong magnetic field as a result of a magnetic breakdown. The cross-sectional areas of these orbits were 1.2 and 6.0% of the cross-sectional area of the Brillouin zone, respectively. The authors of [23] performed experiments at a pressure as high as 1 GPa and found that the topology of the Fermi surface in these crystals did not change with pressure and that the frequencies of the Fourier components of the Shubnikov–de Haas oscillations increased monotonically and reached $F_a = 71$ T and $F_b = 350$ T at the maximum pressure. We could assume that the Fermi surface in our samples has the same topology but slightly different sizes, which results in the two frequencies of Shubnikov–de Haas oscillations that correspond to the closed cross sections detected as a result of a magnetic breakdown in the experiments of [21, 23]. Then, comparing the oscillation frequencies in our samples and the samples from [23] under pressure, we could conclude that the substitution of the DCB solvent for DMF leads to the compression of the lattice that corresponds to an applied pressure of slightly above 1 GPa. However, as shown above, this effect cannot be reduced to chemical compression, and the scenario of the structural reconstruction is more complex.

ACKNOWLEDGMENTS

We thank H. Akutsu and A. Kobayashi for the structural information (CIF file) on β"-(BEDT–TTF)$_4$Rb[Fe(C_2O_4)$_3$] · PYR.

This work was supported by the Russian Foundation for Basic Research (project no. 07-03-91207) and a program of the Presidium of the Russian Academy of Sciences.

REFERENCES

1. T. Ishiguro, K. Yamaji, and G. Saito, *Organic Superconductors*, Ed. by P. Fulde, 2nd ed. (Springer, Berlin, 1998).
2. A. W. Graham, M. Kurmoo, and P. Day, Chem. Commun., 2061 (1995).
3. M. Kurmoo, A. W. Graham, P. Day, et al., J. Am. Chem. Soc. **117**, 12209 (1995).
4. P. Day and M. Kurmoo, Synth. Met. **85**, 1445 (1997).
5. L. Martin, S. S. Turner, P. Day, et al., Chem. Commun., 1367 (1997).
6. L. Martin, S. S. Turner, and P. Day, Synth. Met. **102**, 1638 (1999).
7. L. Martin, S. S. Turner, P. Day, et al., Inorg. Chem. **40**, 1363 (2001).
8. S. Rashid, S. S. Turner, P. Day, et al., Synth. Met. **120**, 985 (2001).
9. S. Rashid, S. S. Turner, P. Day, et al., J. Mater. Chem. **11**, 2095 (2001).
10. H. Akutsu, A. Akutsu-Sato, S. S. Turner, et al., J. Am. Chem. Soc. **124**, 12430 (2002).
11. H. Akutsu, A. Akutsu-Sato, S. S. Turner, et al., Synth. Met. **137**, 1239 (2003).
12. S. S. Turner, P. Day, K. M. A. Malik, et al., Inorg. Chem. **38**, 3543 (1999).
13. A. Akutsu-Sato, A. Kobayashi, T. Mori, et al., Synth. Met. **152**, 373 (2005).
14. S. Rashid, S. S. Turner, D. Le Pevelen, et al., Inorg. Chem. **40**, 5304 (2001).
15. T. G. Prokhorova, S. S. Khasanov, L. V. Zorina, et al., Adv. Funct. Mater. **13**, 403 (2003).
16. L. V. Zorina, S. S. Khasanov, and R. P. Shibaeva, Vestn. Nizhegorod. Univ. im. N. I. Lobachevskogo, Fiz. Tverd. Tela **1** (7), 62 (2004).
17. R. B. Morgunov, A. A. Baskakov, L. R. Dunin-Barkovskiĭ, et al., Khim. Fiz. **24**, 116 (2005).
18. E. Coronado, S. Curelli, C. Giménez-Saiz, and C. J. Gómez-García, Synth. Met. **154**, 245 (2005).
19. E. Coronado, S. Curelli, C. Giménez-Saiz, and C. J. Gómez-García, J. Mater. Chem. **15**, 1429 (2005).
20. A. F. Bangura, A. I. Coldea, J. Singleton, et al., Synth. Met. **137**, 1313 (2003).
21. A. Audouard, V. N. Laukhin, L. Brossard, et al., Phys. Rev. B **69**, 144523 (2004).
22. A. F. Bangura, A. I. Coldea, J. Singleton, et al., Phys. Rev. B **72**, 014543 (2005).
23. A. Audouard, V. N. Laukhin, J. Beard, et al., Phys. Rev. B **74**, 233104 (2006).
24. A. I. Coldea, A. F. Bangura, J. Singleton, et al., Phys. Rev. B **69**, 085112 (2004).
25. D. Vignolles, V. N. Laukhin, A. Audouard, et al., Eur. Phys. J. B **51**, 53 (2006).
26. A. I. Coldea, A. F. Bangura, J. Singleton, et al., J. Low Temp. Phys. **142**, 253 (2007).
27. G. M. Sheldrick, *SHELX97: Programs for Crystal Structure Analysis (Release 97-2)* (Univ. of Göttingen, Germany, 1997).
28. I. J. Bruno, J. C. Cole, P. R. Edgington, et al., Acta Crystallogr. B **58**, 389 (2002).

Translated by K. Shakhlevich